2009

CO chemisorption on the surfaces of the golden cages

Wei Huang
Washington State University, 2710 University Drive, Richland, Washington

Satya S. Bulusu
University of Nebraska-Lincoln, sbulusu@iiti.ac.in

Rhitankar Pal
University of Nebraska - Lincoln

Xiao Cheng Zeng
University of Nebraska-Lincoln, xzeng1@unl.edu

Lai-Sheng Wang
University of Nebraska - Lincoln

CO chemisorption on the surfaces of the golden cages

Wei Huang,[1] Satya Bulusu,[2] Rhitankar Pal,[2] Xiao Cheng Zeng,[2,a)] and Lai-Sheng Wang[3,a)]
[1]*Department of Physics, Washington State University, 2710 University Drive, Richland, Washington 99354, USA and Chemical and Materials Sciences Division, Pacific Northwest National Laboratory, MS K8-88, P. O. Box 999, Richland, Washington 99352, USA*
[2]*Department of Chemistry and Center for Materials and Nanoscience, University of Nebraska-Lincoln, Lincoln, Nebraska 68588, USA*
[3]*Department of Chemistry, Brown University, Providence, Rhode Island 02912, USA*

(Received 16 October 2009; accepted 20 November 2009; published online 18 December 2009)

We report a joint experimental and theoretical study of CO chemisorption on the golden cages. We find that the Au_{17}^- cage is highly robust and retains its cage structure in $Au_{17}(CO)^-$. On the other hand, the Au_{16}^- cage is transformed to a structure similar to Au_{17}^- upon the adsorption of CO. Au_{18}^- is known to consist of two nearly degenerate structures, i.e., a cage and a pyramidal isomer, which coexist in the cluster beam. However, upon CO chemisorption only the cage isomer is observed while the pyramidal isomer no longer exists due to its less favorable interaction with CO, compared to the cage isomer. We find that inclusion of the spin-orbit effects is critical in yielding simulated spectra in quantitative agreement with the experimental data and providing unequivocal structural information and molecular insights into the chemical interactions between CO and the golden cages. © *2009 American Institute of Physics*. [doi:10.1063/1.3273326]

I. INTRODUCTION

The discovery of catalytic effects of gold nanoparticles[1] has stimulated intense interests in the structures and properties of gaseous gold nanoclusters. The structures of gold anion clusters (Au_n^-) with $n=3-20$ have been extensively studied through combined experimental techniques and density
functional theory (DFT) calculations.[2–16] Small Au_n^- clusters ($n<12$) were found to exhibit planar structures.[4,6,17] Au_{12}^- was found to be the critical size for the two-dimensional (2D) to three-dimensional (3D) structural transition:[11,13] the global-minimum structure of Au_{12}^- is 3D with a nearly degenerate 2D isomer coexisting in the cluster beam. Among the small gold clusters, the most interesting structures are the golden pyramid Au_{20}^- (Ref. 5) and the golden cages Au_n^- ($n=16-18$).[9] Recently, using Ar tagging and O_2 titration we found that the cage-to-pyramid transition occurs at Au_{18}^-, for which the cage and pyramidal isomers are nearly degenerate and coexist in the cluster beam.[14]

Among the golden cages, Au_{16}^- has the highest symmetry (T_d) with a diameter about 5.5 Å,[9] suggesting possibilities of endohedral doping in analogy to the endohedral carbon fullerenes. Numerous theoretical and experimental studies of doped golden cages have been reported.[18–26] The first experimental evidence of endohedral doping of the golden cages was achieved with Cu in the $Cu@Au_{16}^-$ and $Cu@Au_{17}^-$ clusters.[20] Photoelectron spectra of the two doped species show striking similarities to those of the parents, suggesting that the Cu dopant induces little distortion to the cages, which is confirmed by theoretical calculations. Further investigations showed that Ag, Zn, In, Fe, Co, and Ni can all be doped into the Au_{16}^- cage, whereas Si, Ge, and Sn disrupt the cage structure.[19,21,25,26]

The interactions of CO with small gold clusters have been the focus of numerous studies because of their implications to the nanogold catalysis for low-temperature CO oxidation.[2,3,27–56] However, the electronic and structural properties of nanoscale $Au_m(CO)_n^-$ clusters are still largely unknown. Recently, Herzing *et al.*[2] proposed that the origin of the catalytic activity of nanogold is associated uniquely with bilayer gold clusters that are ~0.5 nm in diameter, i.e., clusters with about 10–20 atoms. Thus, understanding how O_2 and CO interact with clusters in this size range is of fundamental importance. Herein we report a joint photoelectron spectroscopic and theoretical study of how CO interacts with the golden cages Au_n^- ($n=16-18$). We find that while the Au_{17}^- cage remains intact in $Au_{17}(CO)^-$ the Au_{16}^- and Au_{18}^- cages undergo some structural changes to optimize the chemical interactions with CO.

II. EXPERIMENTAL METHOD

The experiment was carried out using our magnetic-bottle photoelectron spectroscopy (PES) apparatus equipped with a laser vaporization cluster source.[57] A gold disk target was vaporized by a pulsed laser to generate a plasma inside a large-waiting-room cluster nozzle. A high-pressure helium carrier gas pulse was delivered to the nozzle simultaneously, cooling the plasma and initiating nucleation. For the CO chemisorption experiment, we used a helium carrier gas seeded with 0.01% CO, which reacts with the gold clusters inside the nozzle to form various $Au_x(CO)_y^-$ complexes. A low CO concentration was used to optimize the formation of one and two CO chemisorbed complexes. Clusters formed inside the nozzle were entrained in the helium carrier gas and

a)Authors to whom correspondence should be addressed. Electronic addresses: xczeng@phase2.unl.edu and lai-sheng_wang@brown.edu.

TABLE I. Experimental VDEs, and the calculated VDEs, C–O vibrational frequencies, and Au–C bond lengths from the global minimum structures of $Au_n(CO)^-$ ($n=16-18$).

Isomer	VDE (exp) (eV)[a]	VDE (theo) (eV)[b]	C–O frequencies (cm^{-1})[c]	Au–C bond lengths (Å)[c]
$Au_{16}(CO)^-$ (C_s) (isomer III)	3.77(3)	3.55	2019.31	1.92
$Au_{17}(CO)^-$ (C_s) (isomer I)	4.08(3)	3.87	2022.30	1.93
$Au_{18}(CO)^-$ (C_s) (isomer I)	3.32(3)	3.25	2013.02	1.92

[a]The number in the parentheses denotes the uncertainty in the last digit.
[b]The VDEs are calculated at the PBE0/CRENBL/SO level of theory.
[c]The vibrational frequencies and the Au–C bond lengths are computed at the PBE/LANL2DZ(2f,g) (for Au: exponents=1.461, 0.498, and 1.218) and 6-31G(d) (for C and O) level of theory.

underwent a supersonic expansion for further cooling. After a skimmer, anions from the collimated cluster beam were extracted at 90° into a time-of-flight mass spectrometer. Clusters of interest were selected by a mass gate and decelerated before being photodetached by a 193 nm laser beam from an ArF excimer laser. Photoelectrons were collected by a magnetic bottle at nearly 100% efficiency into a 3.5-m-long electron flight tube for kinetic energy analyses. The photoelectron kinetic energies were calibrated by the known spectra of Au^- and subtracted from the photon energies to obtain the reported electron binding energy spectra. The electron kinetic energy (E_k) resolution of our apparatus is $\Delta E_k/E_k \sim 2.5\%$, i.e., ~25 meV for 1 eV electrons. As we showed previously, the temperature of cluster anions is vital in determining the quality of PES spectra. Cold clusters yield much better resolved spectra by eliminating vibrational hot bands or low-lying isomers. We found that by carefully controlling the resident time of the clusters in the nozzle we can produce much colder clusters.[58]

III. THEORETICAL METHODS

To search for low-lying structures of $Au_n(CO)^-$ ($n=16-18$), we employed the basin-hopping global optimization technique coupled with DFT geometry optimization. Generalized gradient approximation in the Perdue–Burke–Ernzerhof (PBE) functional form[59] was employed. Several randomly selected initial structures were used for the basin-hopping searches, all leading to consistent sets of low-lying isomers for each species. These low-lying isomers were re-optimized using the PBE functional and triple zeta 1 polarization function (TZP) basis set, implemented in the ADF 2008.01 software package.[60]

To account for the spin-orbit (SO) effects for computing the simulated spectra, the PBE0 functional and CRENBL basis set (i.e. the large effective-core-potential orbital basis for use with the small core potentials due to Christiansen *et al.*[61]), implemented in NWCHEM 5.1.1,[62,63] were used. The first vertical detachment energies (VDEs) of the anion clusters were computed using delta-self-consistent field (SCF) method at PBE0/CRENBL/SO level (see Table I). The binding energies of deeper orbitals were then added to the first VDE to give VDEs to the excited states. Each VDE was fitted with a Gaussian of width 0.04 eV to yield the simulated spectra. We noted that the PBE0/CRENBL/SO calculations were computationally very demanding. Hence, to compute the vibrational frequencies of the lowest-energy isomers, we used a less expensive level of theory, namely, the PBE functional and LANL2DZ(2f,g) (for Au: exponents=1.461, 0.498, and 1.218) and 6-31G(d) (for C and O) basis set (where LANL2DZ stands for Los Alamos National Laboratory 2-double-zeta), implemented in the GAUSSIAN03 package.[64] Vibrational frequencies and the Au–C bond lengths are also given in Table I.

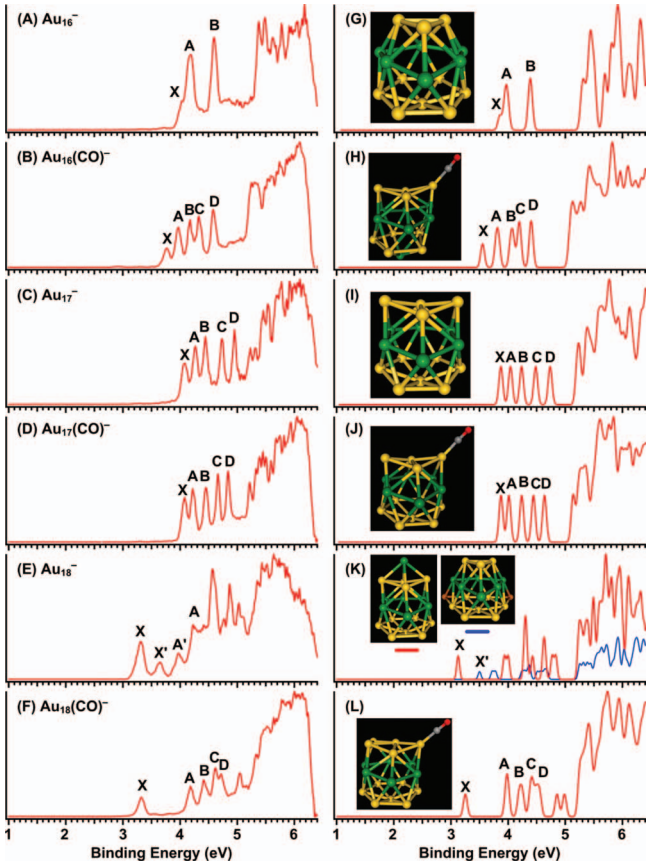

FIG. 1. The experimental (left column) and simulated photoelectron spectra (right column) of $Au_n(CO)^-$ ($n=16-18$) compared with the corresponding Au_n^- clusters. The inset shows the global minimum structures and a low-lying isomer for Au_{18}^-: Au atoms are color coded in yellow and green to aid visualization; C is in gray and O is in red.

IV. RESULTS AND DISCUSSION

A. Experimental photoelectron spectra of $Au_n(CO)^-$ ($n=16-18$)

Figure 1 (left column) shows the 193 nm photoelectron spectra of $Au_n(CO)^-$ ($n=16-18$) produced using helium carrier gas seeded with 0.01% CO, in comparison with those of the corresponding bare Au_n^- clusters. The photoelectron spectrum of $Au_{16}(CO)^-$ [Fig. 1(b)] differs significantly from that of Au_{16}^- [Fig. 1(a)], indicating that CO has induced geometry changes in the golden cage. Walter and Häkkinen[18] used the electron shell model to rationalize the high stability of the Au_{16}^{2-} cage with three filled electron shells,

$1s^2 1p^6 1d^{10}$. The $1d$ shell transforms into t_2 and e molecular orbitals (MOs) under the T_d symmetry with t_2 being the highest occupied MO (HOMO). The t_2 orbital splits into two peaks [X and A, Figs. 1(a) and 1(g)] due to the SO effects. There are, in total, nine electrons involved in the first three peaks of Au_{16}^- (X, A, and B). Interestingly, five distinct peaks are observed for $Au_{16}(CO)^-$ [X, A–D, Fig. 1(b)] in the low binding energy range, as if the A and B bands in the spectrum of Au_{16}^- [Fig. 1(a)] has each split into two bands. This observation suggests that the T_d structure of Au_{16}^- is likely distorted to a lower symmetry in $Au_{16}(CO)^-$, so that the t_2 and e orbitals are split into five nondegenerate orbitals with only one electron in the HOMO. The single occupancy in the HOMO is consistent with the lower relative intensity of the X band in the spectrum of $Au_{16}(CO)^-$ [Fig. 1(b)].

The spectrum of $Au_{17}(CO)^-$ [Fig. 1(d)] is similar to that of the parent Au_{17}^- [Fig. 1(c)], suggesting that CO induces little geometry change in the Au_{17}^- cage. Notably, the spectrum of $Au_{17}(CO)^-$ displays similarities to that of $Au_{16}(CO)^-$ in the low binding energy range, except that the relative intensity of the X band in the former is stronger because $Au_{17}(CO)^-$ is a closed-shell system and its HOMO should be filled with two electrons. The similarities between the spectra of $Au_{16}(CO)^-$ and $Au_{17}(CO)^-$ imply that these two clusters may possess similar cage structures. The spectrum of $Au_{18}(CO)^-$ [Fig. 1(f)] appears simpler than that of Au_{18}^- [Fig. 1(e)]: The X′ and A′ bands disappear while the X and A bands are similar to those for the bare cluster. We have recently shown that for Au_{18}^- both the cage and pyramidal isomers coexist in the cluster beam.[14] In the spectrum of Au_{18}^- [Fig. 1(e)], the X and A bands correspond to the cage isomer while the X′ and A′ bands come from the pyramidal isomer [Fig. 1(k)]. The spectrum of $Au_{18}(CO)^-$ suggests that the pyramidal isomer no longer exists in the cluster beam upon CO chemisorption.

The measured first VDEs for $Au_n(CO)^-$ (n=16–18) are given in Table I. As can be seen in Fig. 1, in addition to the spectral pattern change, CO also induces a significant reduction in electron binding energies in $Au_{16}(CO)^-$ relative to the corresponding bare cluster. On the other hand, both the spectral pattern and electron binding energies of $Au_{17}(CO)^-$ and $Au_{18}(CO)^-$ are similar to their respective bare gold clusters.

B. Computational studies and importance of SO effects

To understand the CO-chemisorption sites in $Au_n(CO)^-$ (n=16–18), we carried out an unbiased search for the global-minimum structures of the chemisorbed complexes using the basin-hopping global optimization technique coupled with DFT geometry optimization. Several randomly constructed initial structures were used and all yielded consistent sets of low-lying isomers. The five lowest-lying isomers of $Au_n(CO)^-$ (n=16–18) at the PBE0/CRENBL/SO level are presented in Fig. 2. The energies of these isomers are all fairly close and in all the isomers CO binds to a low-coordinate apex site, as observed in smaller clusters.

Due to the strong relativistic and SO effects of gold,[65] determination of global minimum structures for gold clusters is extremely challenging. Comparison with experimental data is a prerequisite for reliable structural assignments. We chose Au_{16}^- to benchmark our theoretical methods because its structure is well established. We examined three different functionals [PBE0, B3LYP (i.e. Becke 3-parameter exchange and Lee–Yang–Parr correlation), and M06-L] using the CRENBL basis set (implemented in NWCHEM 5.1.1), and simulated the PES spectrum of Au_{16}^- with and without inclusion of the SO effects, as shown in Fig. 3. We found that the inclusion of the SO effects is critical to yield reliable theoretical data to be compared to the experiment. Both the PBE0 and B3LYP functionals with the SO effects give simulated spectra [Figs. 3(b) and 3(c)] in excellent agreement with the experimental data [Fig. 3(a)]. Even though the computed VDEs are systematically lower relative to the experimental spectrum, the overall spectral patterns at both the PBE0/SO and B3LYP/SO levels are in *quantitative* agreement with the experimental spectrum. We chose the PBE0 functional in the current study because it is computationally more efficient than the B3LYP functional. To further validate the PBE0/CRENBL/SO method, we also recomputed the spectra for the Au_{17}^- and Au_{18}^- clusters [Figs. 1(i) and 1(k)]. We found that the simulated spectra with SO effects for these clusters are also in quantitative agreement with the experimental data and are significantly improved relative to those reported previously without the inclusion of the SO effects.[9,14] This level of agreement between the simulated and experimental data is gratifying, giving us considerable confidence in elucidating the CO-chemisorbed clusters.

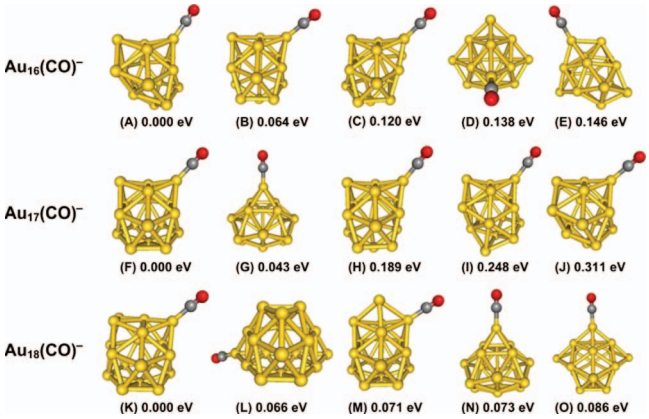

FIG. 2. The structures of the top five low-lying isomers for $Au_n(CO)^-$ (n=16–18), ranked according to their relative energies calculated at PBE0/CRENBL/SO level of theory including the SO effects.

C. Comparison between experimental and simulated photoelectron spectra for $Au_n(CO)^-$ (n=16–18)

We used the same level of theory to compute the spectra of $Au_n(CO)^-$ (n=16–18). Because the relative energies of the low-lying isomers are fairly close for all three chemisorbed complexes, comparisons between the simulated and experimental spectra are essential in determining the true global minimum structures in each case. The simulated spectra for all five low-lying isomers are given in Figs. S1–S3 (Ref. 66) for n=16–18, respectively, where the isomers are also labeled from I to V according to the order given in Fig.

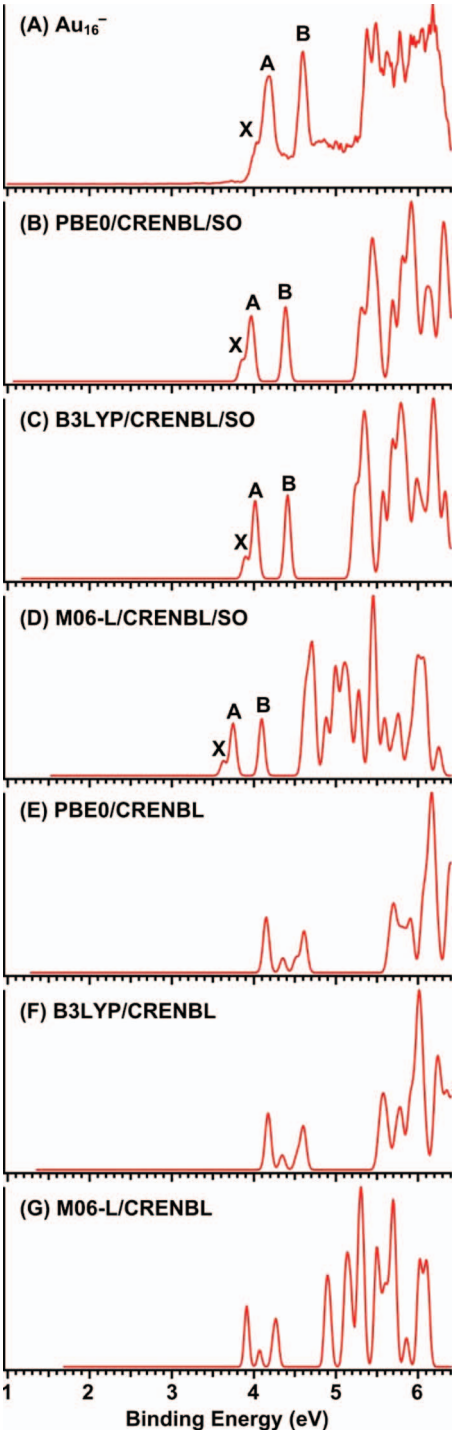

FIG. 3. The simulated photoelectron spectra of Au_{16}^- at different levels of theory in comparison with the experimental spectrum.

2 for easy reference. The simulated spectra and the isomers that yield the best agreement with the experimental data are presented in Fig. 1 (right column). The computed first VDEs are compared with the experimental data in Table I and they are all slightly underestimated.

Our calculations show that the T_d cage structure of Au_{16}^- is significantly distorted in all the low-lying isomers [Figs. 2 and S1]. Isomers II and III are similar and they still possess cage structures. But their detailed atomic positions are different, yielding quite different simulated spectra [Fig. S1]. Among the five low-lying isomers, only the simulated spectra of isomers III and V are in good agreement with the experiment [Figs. S1B and E]. However, isomer V is slightly higher in energy at PBE0/SO level than isomer III by 0.026 eV. In view of the intrinsic error in DFT calculation (typically several meV per atom), we also computed relative energies for isomers of $Au_{16}(CO)^-$ using the hybrid functional B3LYP. Again, at the B3LYP/SO level, isomer V is higher in energy than isomer III by 0.1 eV, consistent with the energy order from PBE0/SO calculation. Thus, on the basis of both the simulated spectrum and the computed energetics, we assigned isomer III as the true global minimum for $Au_{16}(CO)^-$, as shown in Fig. 1(h).

In the global minimum of $Au_{17}(CO)^-$, the cage structure of the parent Au_{17}^- is intact and its simulated spectrum [Figs. 1(j) and S2] is also similar to that of the parent gold cluster, in excellent agreement with the experimental observation (Fig. 1). Thus, there is no ambiguity in the assignment of the global minimum of $Au_{17}(CO)^-$. The global minimum structure of $Au_{18}(CO)^-$ is also a cage, which is slightly changed from the parent Au_{18}^- cage. The simulated spectrum is in excellent agreement with the measured spectrum of $Au_{18}(CO)^-$. In isomer III of $Au_{18}(CO)^-$, the parent cage is not perturbed but its simulated spectrum in terms of peak spacing does not agree with the experimental spectrum as well as isomer I. Isomer II of $Au_{18}(CO)^-$ corresponds to the pyramidal isomer of the parent Au_{18}^- [Fig. 1(k)]. However, comparison of its simulated spectrum [Fig. S3b] to the experiment suggests that this isomer is not present in the experimental spectrum, unlike the bare Au_{18}^- cluster [Figs. 1(e) and 1(k)]. Apparently, the pyramidal isomer does not bind CO as strong as the cage structure in isomer I.

D. Structural evolution and the interactions of CO with Au in $Au_n(CO)^-$ (n=16–18)

The structure of $Au_{16}(CO)^-$ can be understood based on the layer model reported recently:[14] The Au_{16} core can be viewed as composed of four layers (4+6+5+1) [inset in Fig. 1(h)], whereas the parent T_d Au_{16}^- can also be viewed as consisting of four layers (3+6+6+1) [inset in Fig. 1(g)]. Interestingly, the top two layers of $Au_{16}(CO)^-$ are very similar to those of $Au_{17}(CO)^-$ [inset in Fig. 1(j)], whose Au_{17} core also consist of four layers (4+6+6+1). Thus, the local structure near CO is almost identical in $Au_{16}(CO)^-$ and $Au_{17}(CO)^-$, consistent with their similar photoelectron spectral features. The Au_{18} core in $Au_{18}(CO)^-$ is also similar to that in $Au_{17}(CO)^-$ except that the top layer of Au_{18} contains five Au atoms [inset in Fig. 1(l)]. Compared to the parent Au_{18}^- cage, CO only induces a relatively minor structural change in $Au_{18}(CO)^-$: the top apex atom in the Au_{18}^- parent cage [inset in Fig. 1(k)] is displaced slightly to form the five atom top layer while the bottom part of the Au_{18}^- cage remains unchanged upon CO adsorption. We found previously that the Au_{18}^- cage isomer is slightly more reactive with O_2 than the pyramidal isomer.[14] The current result shows that the cage isomer is also more reactive toward CO.

To assess the relative strength of the interactions between CO and the golden cages, we first computed the vi-

brational frequency of CO and the Au–C bond length in $Au_n(CO)^-$, as shown in Table I. The vibrational frequency of CO in $Au_{17}(CO)^-$ is slightly higher than that in $Au_{16}(CO)^-$ and $Au_{18}(CO)^-$, suggesting weaker interactions between CO and Au_{17}^-. Au_{17}^- is closed shell with 18 valence electrons and represents a stable electronic system. Thus, its weaker interaction with CO is understandable and is consistent with the fact that CO also has the least perturbation to the parent Au_{17}^- cage in the chemisorbed complex. For $Au_{18}(CO)^-$, we also computed the CO vibrational frequency and Au–C bond length for the pyramidal isomer [Fig. 2(l)]. They are 2015 cm^{-1} and 1.94 Å, respectively, both of which are larger in comparison to the corresponding values for the cage structure. In addition, we computed basis set superposition error corrected binding energies between CO and the two isomers of Au_{18}^-, respectively. Indeed, we find that the CO binds to the Au_{18}^- cage isomer stronger than to the Au_{18}^- pyramidal isomer. The binding energy between CO and the Au_{18}^- cage is 1.098 eV, while that between CO and the Au_{18}^- pyramid is 0.837 eV [calculated at the PBE/LANL2DZ(2f,g) (for Au: exponents=1.461, 0.498, and 1.218) and 6-31G(d) (for C and O) level of theory]. These results show that the CO interactions with the Au_{18}^- pyramidal isomer are less favorable than with the Au_{18}^- cage isomer. Hence, the population of the $Au_{18}(CO)^-$ cage isomers is expected to be dominating in the cluster beam.

CO is known to prefer low-coordination apex sites on small planer gold cluster anions. However, on the surface of the Au_{16}^- cage, there is no such site because of its high symmetry, which explains the structural distortion in $Au_{16}(CO)^-$. A careful examination of the global minimum structures of all three $Au_n(CO)^-$ chemisorbed complexes reveals a common feature: the CO chemisorption site all involves the apex site of a local square pyramidal unit. Such a square pyramidal site seems to be the favorite CO chemisorption site on the golden cage surfaces and provides the driving force for the structural transformation in the Au cluster core of $Au_{16}(CO)^-$ and $Au_{18}(CO)^-$. On the surface of the Au_{17}^- golden cage, there are already two such square pyramidal sites for CO, which in turn induces little structural change. On the surface of both $Au_{16}(CO)^-$ and $Au_{17}(CO)^-$ there is one more square pyramidal site, which should be a good site for a second CO molecule. Indeed, experimental photoelectron spectra of $Au_{16}(CO)_2^-$ [Fig. S4] (Ref. 66) and $Au_{17}(CO)_2^-$ [Fig. S5] (Ref. 66) are found to be similar to their corresponding monocarbonyl complexes, whereas the spectrum of $Au_{18}(CO)_2^-$ [Fig. S6] (Ref. 66) is found to be different from that of $Au_{18}(CO)^-$ because it lacks a second square pyramidal site for CO. The current study shows that CO chemisorption on the golden cage surfaces is highly site specific, which may have implications to understanding the catalytic effect of nanogold.

V. CONCLUSIONS

In this work, we show that the gold cages Au_{16}^- and Au_{18}^- undergo a cage-to-cage structural transformation upon CO binding. Au_{18}^- is known to consist of two nearly degenerate structures, i.e., a cage and a pyramidal isomer, which coexist in the cluster beam. Upon CO chemisorption only the cage isomer survives while the pyramidal isomer no longer exists due to its less favorable interaction with CO compared to the cage isomer. Interestingly, the Au_{17}^- cage is highly robust and retains its cage structure in $Au_{17}(CO)^-$. It is worth noting that the neutral golden cage Au_{17} has the same cage structure as the anion counterpart,[67] providing further evidence of the robustness of the Au_{17}^- cage structure. In the theoretical calculations of the density of states, we find that inclusion of the SO effects is critical in yielding simulated spectra in quantitative agreement with the experimental data. Such quantitative agreement provides unequivocal structural information, thereby molecular insights into the chemical interactions between CO and the golden cages. In closing, we note that the surfaces of the carbon fullerene cages can be modified to form a variety of new exohedral fullerene molecules. Our joint study demonstrates also that the golden cages can be chemically modified to form new exohedral cage molecules as well.

ACKNOWLEDGMENTS

W.H. would like to thank Dr. Niranjan Govind for invaluable discussions of spin-orbit DFT calculations in NWCHEM. The experimental work and NWChem calculations done at Washington were supported by the National Science Foundation (Grant No. CHE-0749496), and was performed at the EMSL, a national scientific user facility sponsored by the DOE's Office of Biological and Environmental Research and located at the Pacific Northwest National Laboratory, operated for DOE by Battelle. The theoretical work done at Nebraska was supported by grants from the National Science Foundation (Grant Nos. CHE-0427746 and DMR-0820521), the Nebraska Research Initiative, and the University of Nebraska Holland Computing Center.

[1] M. Haruta, Catal. Today **36**, 153 (1997).
[2] A. A. Herzing, C. J. Kiely, A. F. Carley, P. Landon, and G. J. Hutchings, Science **321**, 1331 (2008).
[3] M. Turner, V. B. Golovko, O. P. H. Vaughan, P. Abdulkin, A. Berenguer-Murcia, M. S. Tikhov, B. F. G. Johnson, and R. M. Lambert, Nature (London) **454**, 981 (2008).
[4] F. Furche, R. Ahlrichs, P. Weis, C. Jacob, S. Gilb, T. Bierweiler, and M. M. Kappes, J. Chem. Phys. **117**, 6982 (2002).
[5] J. Li, X. Li, H. J. Zhai, and L. S. Wang, Science **299**, 864 (2003).
[6] H. Häkkinen, B. Yoon, U. Landman, X. Li, H. J. Zhai, and L. S. Wang, J. Phys. Chem. A **107**, 6168 (2003).
[7] E. M. Fernández, J. M. Soler, I. L. Garzón, and L. C. Balbás, Phys. Rev. B **70**, 165403 (2004).
[8] X. Xing, B. Yoon, U. Landman, and J. H. Parks, Phys. Rev. B **74**, 165423 (2006).
[9] S. Bulusu, X. Li, L. S. Wang, and X. C. Zeng, Proc. Natl. Acad. Sci. U.S.A. **103**, 8326 (2006).
[10] B. Yoon, P. Koskinen, B. Huber, O. Kostko, B. von Issendorff, H. Häkkinen, M. Moseler, and U. Landman, ChemPhysChem **8**, 157 (2007).
[11] M. P. Johansson, A. Lechtken, D. Schooss, M. M. Kappes, and F. Furche, Phys. Rev. A **77**, 053202 (2008).
[12] H. Häkkinen, Chem. Soc. Rev. **37**, 1847 (2008).
[13] W. Huang and L. S. Wang, Phys. Rev. Lett. **102**, 153401 (2009).
[14] W. Huang, S. Bulusu, R. Pal, X. C. Zeng, and L. S. Wang, ACS Nano **3**, 1225 (2009).
[15] W. Huang and L. S. Wang, Phys. Chem. Chem. Phys. **11**, 2663 (2009).
[16] A. Lechtken, C. Neiss, M. M. Kappes, and D. Schooss, Phys. Chem. Chem. Phys. **11**, 4344 (2009).
[17] H. Häkkinen, M. Moseler, and U. Landman, Phys. Rev. Lett. **89**, 033401 (2002).

[18] M. Walter and H. Häkkinen, Phys. Chem. Chem. Phys. **8**, 5407 (2006).
[19] Q. Sun, Q. Wang, G. Chen, and P. Jena, J. Chem. Phys. **127**, 214706 (2007).
[20] L. M. Wang, S. Bulusu, H. J. Zhai, X. C. Zeng, and L. S. Wang, Angew. Chem., Int. Ed. **46**, 2915 (2007).
[21] L. M. Wang, S. Bulusu, W. Huang, R. Pal, L. S. Wang, and X. C. Zeng, J. Am. Chem. Soc. **129**, 15136 (2007).
[22] W. Fa and A. P. Yang, Phys. Lett. A **372**, 6392 (2008).
[23] W. Fa and J. M. Dong, J. Chem. Phys. **128**, 144307 (2008).
[24] Q. Sun, Q. Wang, P. Jena, and Y. Kawazoe, ACS Nano **2**, 341 (2008).
[25] L. M. Wang, J. Bai, A. Lechtken, W. Huang, D. Schooss, M. M. Kappes, X. C. Zeng, and L. S. Wang, Phys. Rev. B **79**, 033413 (2009).
[26] L. M. Wang, R. Pal, W. Huang, X. C. Zeng, and L. S. Wang, J. Chem. Phys. **130**, 051101 (2009).
[27] Q. Sun, P. Jena, Y. D. Kim, M. Fischer, and G. Gantefor, J. Chem. Phys. **120**, 6510 (2004).
[28] H. J. Zhai and L. S. Wang, J. Chem. Phys. **122**, 051101 (2005).
[29] H. J. Zhai, B. Kiran, B. Dai, J. Li, and L. S. Wang, J. Am. Chem. Soc. **127**, 12098 (2005).
[30] U. Landman, B. Yoon, C. Zhang, U. Heiz, and M. Arenz, Top. Catal. **44**, 145 (2007).
[31] H. J. Zhai, L. L. Pan, B. Dai, B. Kiran, J. Li, and L. S. Wang, J. Phys. Chem. C **112**, 11920 (2008).
[32] D. Stolcic, M. Fischer, G. Gantefor, Y. D. Kim, Q. Sun, and P. Jena, J. Am. Chem. Soc. **125**, 2848 (2003).
[33] M. L. Kimble, A. W. Castleman, R. Mitric, C. Burgel, and V. Bonačić-Koutecký, J. Am. Chem. Soc. **126**, 2526 (2004).
[34] J. Hagen, L. D. Socaciu, M. Elijazyfer, U. Heiz, T. M. Bernhardt, and L. Wöste, Phys. Chem. Chem. Phys. **4**, 1707 (2002).
[35] L. D. Socaciu, J. Hagen, T. M. Bernhardt, L. Wöste, U. Heiz, H. Häkkinen, and U. Landman, J. Am. Chem. Soc. **125**, 10437 (2003).
[36] W. T. Wallace and R. L. Whetten, J. Phys. Chem. B **104**, 10964 (2000).
[37] W. T. Wallace and R. L. Whetten, J. Am. Chem. Soc. **124**, 7499 (2002).
[38] W. T. Wallace, R. B. Wyrwas, A. J. Leavitt, and R. L. Whetten, Phys. Chem. Chem. Phys. **7**, 930 (2005).
[39] M. A. Nygren, P. E. M. Siegbahn, C. Jin, T. Guo, and R. E. Smalley, J. Chem. Phys. **95**, 6181 (1991).
[40] T. H. Lee and K. M. Ervin, J. Phys. Chem. **98**, 10023 (1994).
[41] N. Veldeman, P. Lievens, and M. Andersson, J. Phys. Chem. A **109**, 11793 (2005).
[42] I. Balteanu, O. P. Balaj, B. S. Fox, M. K. Beyer, Z. Bastl, and V. E. Bondybey, Phys. Chem. Chem. Phys. **5**, 1213 (2003).
[43] M. Neumaier, F. Weigend, O. Hampe, and M. M. Kappes, J. Chem. Phys. **122**, 104702 (2005).
[44] A. Fielicke, G. von Helden, G. Meijer, D. B. Pedersen, B. Simard, and D. M. Rayner, J. Am. Chem. Soc. **127**, 8416 (2005).
[45] A. Fielicke, G. von Helden, G. Meijer, B. Simard, and D. M. Rayner, J. Phys. Chem. B **109**, 23935 (2005).
[46] G. Lüttgens, N. Pontius, P. S. Bechthold, M. Neeb, and W. Eberhardt, Phys. Rev. Lett. **88**, 076102 (2002).
[47] H. Häkkinen and U. Landman, J. Am. Chem. Soc. **123**, 9704 (2001).
[48] B. Yoon, H. Häkkinen, and U. Landman, J. Phys. Chem. A **107**, 4066 (2003).
[49] X. Wu, L. Senapati, S. K. Nayak, A. Selloni, and M. Hajaligol, J. Chem. Phys. **117**, 4010 (2002).
[50] S. A. Varganov, R. M. Olson, M. S. Gordon, and H. Metiu, J. Chem. Phys. **119**, 2531 (2003).
[51] S. A. Varganov, R. M. Olson, M. S. Gordon, G. Mills, and H. Metiu, Chem. Phys. Lett. **368**, 778 (2003).
[52] G. Mills, M. S. Gordon, and H. Metiu, Chem. Phys. Lett. **359**, 493 (2002).
[53] R. Mitric, C. Brgel, and V. Bonaic-Koutecky, Proc. Natl. Acad. Sci. U.S.A. **104**, 10314 (2007).
[54] D. W. Yuan and Z. Zeng, J. Chem. Phys. **120**, 6574 (2004).
[55] X. Ding, Z. Li, J. Yang, J. G. Hou, and Q. Zhu, J. Chem. Phys. **120**, 9594 (2004).
[56] S. Sicolo, L. Giordano, and G. Pacchioni, J. Phys. Chem. C **113**, 10256 (2009).
[57] L. S. Wang, H. S. Cheng, and J. W. Fan, J. Chem. Phys. **102**, 9480 (1995).
[58] J. Akola, M. Manninen, H. Häkkinen, U. Landman, X. Li, and L. S. Wang, Phys. Rev. B **60**, R11297 (1999).
[59] J. P. Perdew, K. Burke, and M. Ernzerhof, Phys. Rev. Lett. **77**, 3865 (1996).
[60] www.scm.com
[61] R. B. Ross, J. M. Powers, T. Atashroo, W. C. Ermler, L. A. LaJohn, and P. A. Christiansen, J. Chem. Phys. **93**, 6654 (1990).
[62] E. J. Bylaska, W. A. d. Jong, N. Govind, K. Kowalski, T. P. Straatsma, M. Valiev, D. Wang, E. Apra, T. L. Windus, J. Hammond, P. Nichols, S. Hirata, M. T. Hackler, Y. Zhao, R. J. H. P.-D. Fan, M. Dupuis, D. M. A. Smith, J. Nieplocha, V. Tipparaju, N. G. W. A. de Jong, R. J. Harrison, M. Dupuis, M. Krishnan, Q. Wu, T. Van Voorhis, A. A. Auer, M. Nooijen, E. Brown, G. Cisneros, G. I. Fann, H. Fruchtl, J. Garza, K. Hirao, R. Kendall, J. A. Nichols, K. Tsemekhman, K. Wolinski, J. Anchell, D. Bernholdt, P. Borowski, T. Clark, D. Clerc, H. Dachsel, M. Deegan, K. Dyall, D. Elwood, E. Glendening, M. Gutowski, A. Hess, J. Jaffe, B. Johnson, J. Ju, R. Kobayashi, R. Kutteh, Z. Lin, R. Littlefield, X. Long, B. Meng, T. Nakajima, S. Niu, L. Pollack, M. Rosing, G. Sandrone, M. Stave, H. Taylor, G. Thomas, J. van Lenthe, A. Wong, and Z. Zhang, *A Computational Chemistry Package for Parallel Computers, Version 5.1.1* (Pacific Northwest National Laboratory, Richland, 2009).
[63] R. A. Kendall, E. Apra, D. E. Bernholdt, E. J. Bylaska, M. Dupuis, G. I. Fann, R. J. Harrison, J. L. Ju, J. A. Nichols, J. Nieplocha, T. P. Straatsma, T. L. Windus, and A. T. Wong, Comput. Phys. Commun. **128**, 260 (2000).
[64] M. J. Frisch, G. W. Trucks, H. B. Schlegel, G. E. Scuseria, M. A. Robb, J. R. Cheeseman, J. J. A. Montgomery, K. N. T. K. Vreven, J. C. Burant, J. M. Millam, S. S. Iyengar, J. Tomasi, V. Barone, B. Mennucci, M. Cossi, G. Scalmani, N. Rega, G. A. Petersson, H. Nakatsuji, M. Hada, M. Ehara, K. Toyota, R. Fukuda, J. Hasegawa, M. Ishida, T. Nakajima, Y. Honda, O. Kitao, H. Nakai, M. Klene, X. Li, J. E. Knox, H. P. Hratchian, J. B. Cross, V. Bakken, C. Adamo, J. Jaramillo, R. Gomperts, R. E. Stratmann, O. Yazyev, A. J. Austin, R. Cammi, C. Pomelli, J. W. Ochterski, P. Y. Ayala, K. Morokuma, G. A. Voth, P. Salvador, J. J. Dannenberg, V. G. Zakrzewski, S. Dapprich, A. D. Daniels, M. C. Strain, O. Farkas, D. K. Malick, A. D. Rabuck, K. Raghavachari, J. B. Foresman, J. V. Ortiz, Q. Cui, A. G. Baboul, S. Clifford, J. Cioslowski, B. B. Stefanov, G. Liu, A. Liashenko, P. Piskorz, I. Komaromi, R. L. Martin, D. J. Fox, T. Keith, M. A. Al-Laham, C. Y. Peng, A. Nanayakkara, M. Challacombe, P. M. W. Gill, B. Johnson, W. Chen, M. W. Wong, C. Gonzalez, and J. A. Pople, GAUSSIAN03, Revision C.02, Gaussian, Inc., Wallingford, CT, 2004.
[65] P. Pyykkö, Chem. Rev. **88**, 563 (1988).
[66] See EPAPS supplementary material at http://dx.doi.org/10.1063/1.3273326 for simulated PES spectra and relative energies of low-lying isomers of $Au_{16}(CO)^-$, $Au_{17}(CO)^-$ and $Au_{18}(CO)^-$, as well as experimental PES spectra of $Au_{16}(CO)_n$, $Au_{17}(CO)_n$, and $Au_{18}(CO)n$ $(n=1-2)$
[67] S. Bulusu and X. C. Zeng, J. Chem. Phys. **125**, 154303 (2006).